A Surgical Guidance System for Big-Bubble Deep Anterior Lamellar Keratoplasty

Hessam Roodaki[1(✉)], Chiara Amat di San Filippo[1], Daniel Zapp[3], Nassir Navab[1,2], and Abouzar Eslami[4]

[1] Computer Aided Medical Procedures, Technische Universität München, Munich, Germany
he.roodaki@tum.de
[2] Computer Aided Medical Procedures, Johns Hopkins University, Baltimore, USA
[3] Augenklinik rechts der Isar, Technische Universität München, Munich, Germany
[4] Carl Zeiss Meditec AG, Munich, Germany

Abstract. Deep Anterior Lamellar Keratoplasty using Big-Bubble technique (BB-DALK) is a delicate and complex surgical procedure with a multitude of benefits over Penetrating Keratoplasty (PKP). Yet the steep learning curve and challenges associated with BB-DALK prevents it from becoming the standard procedure for keratoplasty. Optical Coherence Tomography (OCT) aids surgeons to carry out BB-DALK in a shorter time with a higher success rate but also brings complications of its own such as image occlusion by the instrument, the constant need to reposition and added distraction. This work presents a novel real-time guidance system for BB-DALK which is practically a complete tool for smooth execution of the procedure. The guidance system comprises of modified 3D+t OCT acquisitions, advanced visualization, tracking of corneal layers and providing depth information using Augmented Reality. The system is tested by an ophthalmic surgeon performing BB-DALK on several *ex vivo* pig eyes. Results from multiple evaluations show a maximum tracking error of 8.8 micrometers.

1 Introduction

Ophthalmic anterior segment surgery is among the most technically challenging manual procedures. Penetrating Keratoplasty (PKP) is a well-established transplant procedure for the treatment of multiple diseases of the cornea. In PKP, the full thickness of the diseased cornea is removed and replaced with a donor cornea that is positioned into place and sutured with stitches. Deep Anterior Lamellar Keratoplasty (DALK) is proposed as an alternative method for corneal disorders not affecting the endothelium. The main difference of DALK compared to PKP is the preservation of the patient's own endothelium. This advantage reduces the risk of immunologic reactions and graft failure while showing similar overall visual outcomes. However, DALK is generally more complicated and time-consuming with a steep learning curve particularly when the host stroma is manually removed layer by layer [4]. In addition, high rate of intraoperative

S. Ourselin et al. (Eds.): MICCAI 2016, Part I, LNCS 9900, pp. 378–385, 2016.
DOI: 10.1007/978-3-319-46720-7_44

perforation keeps DALK from becoming surgeons' method of choice [7]. To overcome the long surgical time and high perforation rate of DALK, in [1] Anwar *et al.* have proposed the big-bubble DALK technique (BB-DALK). The fundamental step of the big-bubble technique is the insertion of a needle into the deep stroma where air is injected with the goal of separating the posterior stroma and the Descemet's Membrane (DM). The needle is intended to penetrate to a depth of more than 60 % of the cornea, where the injection of air in most cases forms a bubble. However, in fear of perforating the DM, surgeons often stop the insertion before the target depth, where air injection results only in diffuse emphysema of the anterior stroma [7]. When bubble formation is not achieved, effort on exposing a deep layer nearest possible to the DM carries the risk of accidental perforation which brings further complications to the surgical procedure.

Optical Coherence Tomography (OCT) has been shown to increase the success rate of the procedure by determining the depth of the cannula before attempting the air injection [2]. Furthermore, recent integration of Spectral Domain OCT (SD-OCT) into surgical microscopes gives the possibility of continuous monitoring of the needle insertion. However, current OCT acquisition configurations and available tools to visualize the acquired scans are insufficient for the purpose. Metallic instruments interfere with the OCT signal leading to obstruction of deep structures. The accurate depth of the needle can only be perceived by removing the needle and imaging the created tunnel since the image captured when the needle is in position only shows the reflection of the top segment of the metallic instrument [2]. Also, limited field of view makes it hard to keep the OCT position over the needle when pressure is applied for insertion.

Here we propose a complete system as a guidance tool for BB-DALK. The system consists of modified 3D+t OCT acquisition using a microscope-mounted scanner, sophisticated visualization, tracking of the epithelium (top) and endothelium (bottom) layers and providing depth information using Augmented Reality (AR). The method addresses all aspects of the indicated complex procedure, hence is a practical solution to improve surgeons' and patients' experience.

2 Method

As depicted in Fig. 1, the system is based on an OPMI LUMERA 700 microscope equipped with a modified integrated RESCAN 700 OCT device (Carl Zeiss Meditec, Germany). A desktop computer with a quad-core Intel Core i7 CPU, a single NVIDIA GeForce GTX TITAN X GPU and two display screens are connected to the OCT device. Interaction with the guidance system is done by the surgeon's assistant via a 3D mouse (3Dconnexion, Germany). The surgeon performs the procedure under the microscope while looking at the screens for both microscopic and OCT feedback. The experiments are performed on *ex vivo* pig eyes as shown in Fig. 3a using 27 and 30 gauge needles. For evaluations, a micromanipulator and a plastic anterior segment phantom eye are used.

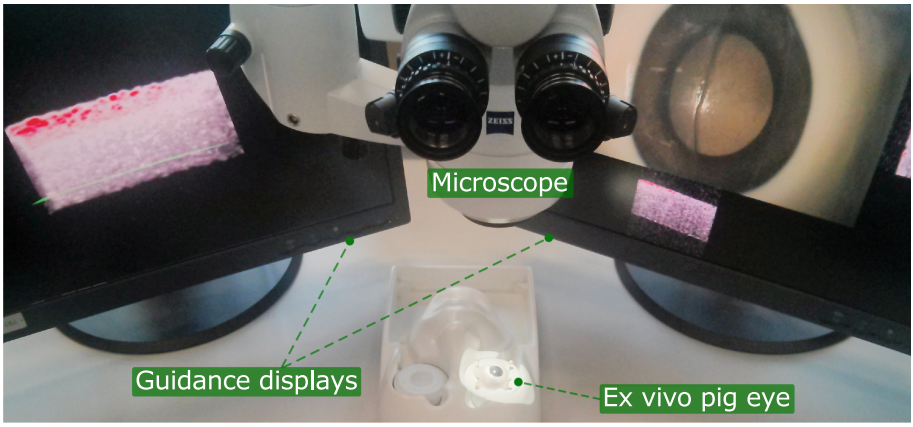

Fig. 1. Experimental setup of the guidance system.

2.1 OCT Acquisition

The original configuration of the intraoperative OCT device is set to acquire B-scans consisting of either 512 or 1024 A-scans. It can be set to acquire a single B-scan, 2 orthogonal B-scans or 5 parallel B-scans. For the proposed guidance system, the OCT device is set to provide 30 B-scans each with 90 A-scan samples by reprogramming the movement of its internal mirror galvanometers. B-scans are captured in a reciprocating manner for shorter scanning time. The scan region covered by the system is 2 mm by 6 mm. The depth of each A-scan is 1024 pixels corresponding to 2 mm in tissue. The concept is illustrated in Fig. 2a.

The cuboid of $30 \times 90 \times 1024$ voxels is scanned at the rate of 10 volumes per second. Since the cuboid is a 3D grid of samples from a continuous scene, it is interpolated using tricubic interpolants to the target resolution of $180 \times 540 \times 180$

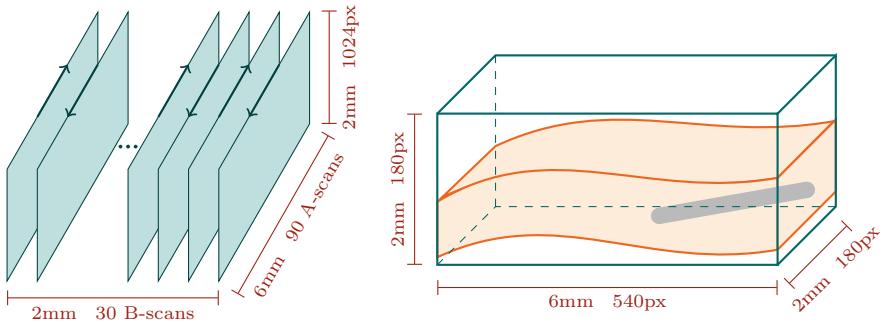

(a) (b)

Fig. 2. (a): The modified pattern of OCT acquisition. (b): The lateral visualization of the cornea (orange) and the surgical needle (gray) in an OCT cuboid.

voxels (Fig. 2b). For that, frames are first averaged along the depth to obtain 30 frames of 90×30 pixels. Then in each cell of the grid, a tricubic interpolant which maps coordinates to intensity values is defined as follows:

$$f(x, y, z) = \sum_{i,j,k=0}^{3} c_{ijk} x^i y^j z^k, \qquad x, y, z \in [0, 1], \tag{1}$$

in which c_{ijk} are the 64 interpolant coefficients calculated locally from the grid sample points and their derivatives. The coefficients are calculated by multiplication of a readily available 64×64 matrix and the vector of 64 elements consisting of 8 sample points and their derivatives [6]. The interpolation is implemented on the CPU in a parallel fashion.

2.2 Visualization

The achieved 3D OCT volume is visualized on both 2D monitors using GPU ray casting with 100 rays per pixel. Maximum information in OCT images is gained from high-intensity values representing boundaries between tissue layers. Hence, the Maximum Intensity Projection (MIP) technique is employed for rendering to put an emphasis on corneal layers. Many segmentation algorithms in OCT imaging are based on adaptive intensity thresholding [5]. Metallic surgical instruments including typical needles used for the BB-DALK procedure have infrared reflectivity profiles that are distinct from cellular tissues. The 3D OCT volume is segmented into the background, the cornea and the instrument by taking advantage of various reflectivity profiles and employing K-means clustering. The initial cluster mean values are set for the background to zero, the cornea to the volume mean intensity (μ) and the instrument to the volume mean intensity plus two standard deviations ($\mu + 2\sigma$). The segmentation is used to dynamically alter the color and opacity transfer functions to ensure the instrument is distinctly and continuously visualized in red, the background speckle noise is suppressed and the corneal tissue opacity does not obscure the instrument (Fig. 3b, c).

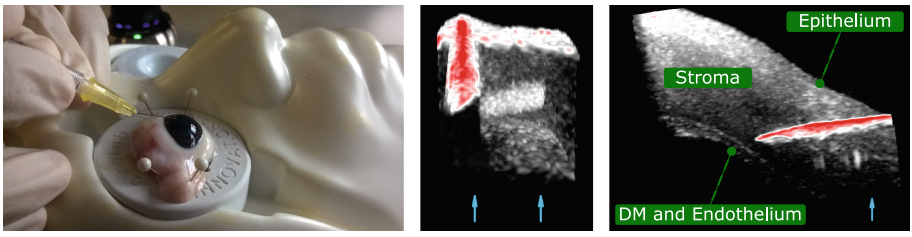

(a) (b) (c)

Fig. 3. (a): Needle insertion performed by the surgeon on the *ex vivo* pig eye. (b), (c): 3D visualization of the OCT cuboid with frontal and lateral viewpoints. The needle is distinctly visualized in red while endothelium (arrow) is not apparent.

The OCT cuboid could be examined from different viewpoints according to the exact need of the surgeon. For this purpose, one of the two displays could be controlled by the surgeon's assistant using a 3D mouse with zooming, panning and 3D rotating functionalities. The proposed guidance system maintains an automatic viewpoint of the OCT volume next to the microscopic view in the second display using the tracking procedure described below.

2.3 Tracking

The corneal DM and endothelial layer are the main targets of the BB-DALK procedure. The DM must not be perforated while the needle must be guided as close as possible to it. However, the two layers combined do not have a footprint larger than a few pixels in OCT images. As an essential part of the guidance system, DM and endothelium 3D surfaces are tracked for continuous feedback by solid visualization. The advancement of the needle in a BB-DALK procedure is examined and reported by percentage of the stroma that is above the needle tip. Hence, the epithelium surface of the cornea is also tracked to assist the surgeon by the quantitative guidance of the insertion.

Tracking in each volume is initiated by detection of the topmost and bottommost 3D points in the segmented cornea of the OCT volume. Based on the spherical shape of the cornea, two half spheres are considered as models of the endothelium and epithelium surfaces. The models are then fitted to the detected point clouds using iterative closest point (ICP) algorithm. Since the insertion of the needle deforms the cornea, ICP is utilized with 3D affine transformation at its core [3]. If the detected and the model half sphere point clouds are respectively denoted as $P = \{p_i\}_{i=1}^{N_P} \in \mathbb{R}^3$ and $M = \{m_i\}_{i=1}^{N_M} \in \mathbb{R}^3$, each iteration of the tracker algorithm is consecutively minimizing the following functions:

$$C(i) = \underset{j \in \{1,\ldots,N_P\}}{\arg\min} \|(A_{k-1}m_i + t_{k-1}) - p_i\|_2^2, \qquad \text{for all } i \in \{1,..,N_M\}. \tag{2}$$

$$(A_k, t_k) = \underset{A,t}{\arg\min} \frac{1}{N} \sum_{i=1}^{N} \|(Am_i + t) - p_{C(i)}\|_2^2. \tag{3}$$

Equation 2 finds the correspondence $C(i)$ between $N \leq min(N_P, N_M)$ detected and model points. Equation 3 minimizes the Euclidean distance between the detected points and the transformed points of the model. A_k and t_k are the desired affine and translation matrices at iteration k. For each incoming volume, ICP is initialized by the transformation that brings the centroid of the model points to the centroid of the detected points. The algorithm stops after 30 iterations.

The lateral view of the OCT volume gives a better understanding of the needle dimensions and advancement. Also, the perception of the distance between the instrument and the endothelium layer is best achieved from viewing the scene parallel to the surface. Therefore, the viewpoint of the second display is constantly kept parallel to a small plane at the center of the tracked endothelium

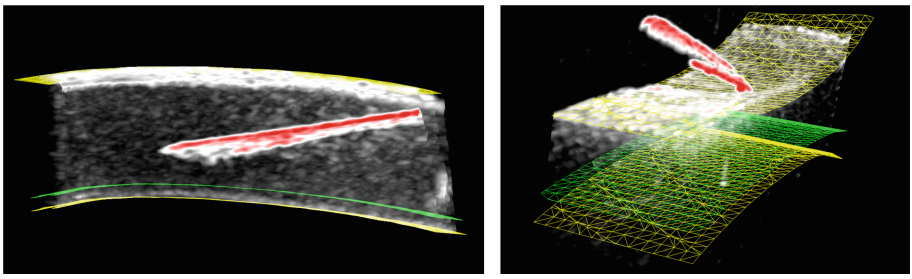

(a) (b)

Fig. 4. Augmented Reality is used to solidly visualize the endothelium and epithelium surfaces (yellow) using wireframes. A hypothetical surface (green) is rendered to indicate the insertion target depth.

surface (Fig. 4a). The pressure applied for insertion of the needle leads to deformation of the cornea. To keep the OCT field of view centered on the focus of the procedure despite the induced shifts, the OCT depth range is continuously centered to halfway between top and bottom surfaces. This is done automatically to take the burden of manual repositioning away from the surgeon.

2.4 Augmented Reality

To further assist the surgeon, a hypothetical third surface is composed between the top and bottom surfaces indicating the insertion target depth (Fig. 4). The surgeon can choose a preferred percentage of penetration at which the imaginary surface would be rendered. Each point of the third surface is a linear combination of the corresponding points on the tracked epithelium and endothelium layers according to the chosen percentage. To visualize the detected surfaces, a wireframe mesh is formed on each of the three point sets. The two detected surfaces are rendered in yellow at their tracked position and the third surface is rendered

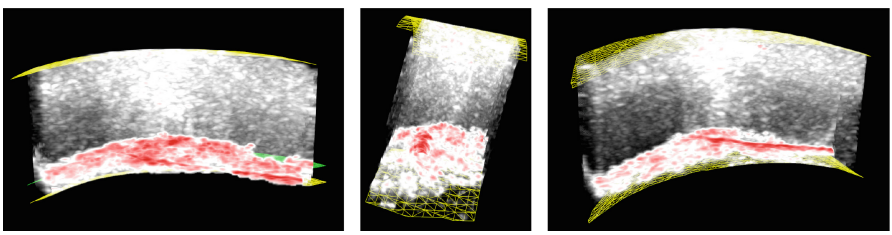

(a) (b) (c)

Fig. 5. Results of air injection in multiple pig eyes visualized from various viewpoints. The concentration of air in the bottommost region of the cornea indicates the high insertion accuracy. Deep stroma is reached with no sign of perforation.

in green at its hypothetical location. Visualization of each surface could be turned off if necessary. After injection, the presence of air leads to high-intensity voxels in the OCT volume. Therefore, the separation region is visualized effectively in red and could be used for validation of separation (Fig. 5).

3 Experiments and Results

The proposed guidance system is tested by an ophthalmic surgeon experienced in corneal transplantation procedure on several *ex vivo* pig eyes. The visualization gives a new dimension never seen before in conventional systems in his comment. His experience with the system signifies the ability of the real-time guidance solution to help in deep needle insertions with fewer perforation incidents.

For the purpose of real-time OCT acquisition, the surgical scene is sparsely sampled via a grid of A-scans and interpolated. To evaluate the accuracy of interpolation against dense sampling, four fixed regions of a phantom eye ($2\,\text{mm} \times 6\,\text{mm} \times 2\,\text{mm}$) are scanned once with real-time sparse sampling ($30\,px \times 90\,px \times 1024\,px$) and two times with slow dense sampling ($85\,px \times 512\,px \times 1024\,px$). The sparse volumes are then interpolated to the size of the dense volumes. Volume pixels have intensities in the range of $[0, 1]$. For each of the four regions, Mean Absolute Error (MAE) of pixel intensities is once calculated for the two dense captures and once for one of the dense volumes and the interpolated volume. A maximum pixel intensity error of 0.073 is observed for the dense-sparse comparison while a minimum pixel intensity error of 0.043 is observed for the dense-dense comparison. The reason for the observed error in dense-dense comparison lies in the presence of OCT speckle noise which is a known phenomenon. The error observed for the dense-sparse comparison is comparable with the error induced by speckle noise hence the loss in sparse sampling is insignificant.

Human corneal thickness is reported to be around $500\,\mu\text{m}$. To ensure a minimum chance of perforation when insertion is done to the depth of 90 %, the tracking accuracy required is around $50\,\mu\text{m}$. To evaluate tracking accuracy of the proposed solution, a micromanipulator with a resolution of $5\,\mu\text{m}$ is used. A phantom eye and a pig eye are fixed to a micromanipulator and precisely moved upwards and downwards while the epithelium and endothelium surfaces are tracked. At each position, the change in the depth of the tracked surfaces corresponding points are studied. Results are presented in Table 1 using box-and-whisker plots. The whiskers are showing the minimum and maximum recorded change of all tracked points while the start and the end of the box are the first and third quartiles. Bands and dots represent medians and means of the recorded changes respectively. The actual value against which the tracking accuracy should be compared is highlighted in red on the horizontal axis of the plots. Overall, the maximum tracking error is $8.8\,\mu\text{m}$.

Table 1. Evaluation of Tracking

Experiment	Actual move (μm)	Detected epithelium displacement (μm)	Detected endothelium displacement (μm)
Phantom eye	10	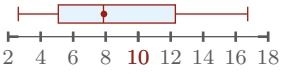	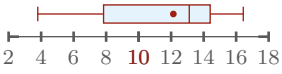
Phantom eye	30	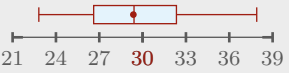	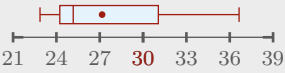
Pig eye	10	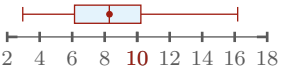	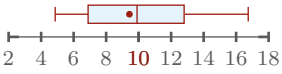
Pig eye	30	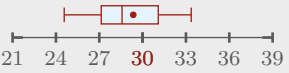	

4 Conclusion

This work presents a novel real-time guidance system for one of the most challenging procedures in ophthalmic microsurgery. The use of medical AR aims at facilitation of the BB-DALK learning process. Experiments on *ex vivo* pig eyes suggest the usability and reliability of the system leading to more effective yet shorter surgery sessions. Quantitative evaluations of the system indicate its high accuracy in depicting the surgical scene and tracking its changes leading to precise and deep insertions. Future work will be in the direction of adding needle tracking and navigation, further evaluations and clinical *in vivo* tests.

References

1. Anwar, M., Teichmann, K.D.: Big-bubble technique to bare Descemet's membrane in anterior lamellar keratoplasty. J. Cataract Refract. Surg. **28**(3), 398–403 (2002)
2. De Benito-Llopis, L., Mehta, J.S., Angunawela, R.I., Ang, M., Tan, D.T.: Intraoperative anterior segment optical coherence tomography: a novel assessment tool during deep anterior lamellar keratoplasty. Am. J. Ophthalmol. **157**(2), 334–341 (2014)
3. Du, S., Zheng, N., Ying, S., Liu, J.: Affine iterative closest point algorithm for point set registration. Pattern Recogn. Lett. **31**(9), 791–799 (2010)
4. Fontana, L., Parente, G., Tassinari, G.: Clinical outcomes after deep anterior lamellar keratoplasty using the big-bubble technique in patients with keratoconus. Am. J. Ophthalmol. **143**(1), 117–124 (2007)
5. Ishikawa, H., Stein, D.M., Wollstein, G., Beaton, S., Fujimoto, J.G., Schuman, J.S.: Macular segmentation with optical coherence tomography. Invest. Ophthalmol. Vis. Sci. **46**(6), 2012–2017 (2005)
6. Lekien, F., Marsden, J.: Tricubic interpolation in three dimensions. Int. J. Numer. Meth. Eng. **63**(3), 455–471 (2005)
7. Scorcia, V., Busin, M., Lucisano, A., Beltz, J., Carta, A., Scorcia, G.: Anterior segment optical coherence tomography-guided big-bubble technique. Ophthalmology **120**(3), 471–476 (2013)